Insertion of Magainin into the Lipid Bilayer Detected Using Lipid Photolabels†

Euijung Jo,‡ Jack Blazyk,§ and Joan M. Boggs*,‡

The Research Institute, The Hospital for Sick Children, Toronto, Canada M5G 1X8, Department of Laboratory Medicine & Pathobiology, University of Toronto, Toronto, Canada M5G 1L5, and Department of Chemistry and Biochemistry, College of Osteopathic Medicine, Ohio University, Athens, Ohio 45701

Received April 16, 1998; Revised Manuscript Received June 23, 1998

ABSTRACT: We investigated the interaction of the antimicrobial peptides Ala_{19}-magainin 2 amide and magainin 2 amide with lipid using two lipid photolabels, azidobenzoyl galactosylceramide (GalCer-PL) and azidobenzoylamido capryloyl galactosylceramide (GalCer-C8-PL), which position their photosensitive groups near the apolar−polar interface and near the center of the bilayer, respectively. Magainins have been postulated to permeabilize membranes either by inserting in a transmembrane fashion into the bilayer and forming a channel or by binding to the surface of the bilayer and disturbing lipid packing. Evidence for channel formation has been difficult to obtain, possibly because only a fraction of the peptide may form a channel at any one time and because the channels may have a short lifetime. Both photolabels significantly labeled the peptides when bound to acidic phospholipid vesicles. The extent of labeling by GalCer-C8-PL was at least 70% of that by GalCer-PL, indicating that some of the peptide was inserted deeply into the bilayer at least transiently. The extent of labeling of Ala_{19}-magainin 2 amide increased significantly with an increase in the peptide to lipid mole ratio, indicating cooperativity and supporting the channel model. The extent of labeling of this peptide was maximal by 30 s and did not change over 30 min, indicating that peptide insertion is rapid and either that the peptide remains inserted for at least 30 min or that equilibrium between inserted and noninserted peptide is achieved by 30 s. The latter is supported by other studies in the literature. Use of this hydrophobic photolabeling technique has permitted detection of peptide monomers which inserted into the bilayer and/or formed a channel at some time during the labeling procedure.

Magainins are peptides isolated from the skin of the African clawed frog, *Xenopus laevis*. They are of interest because they show broad spectrum antimicrobial (*1*−*3*) and anti-cancer cell (*4*, *5*) activities at concentrations which are not hemolytic. Their antimicrobial activity is due to their ability to permeabilize membranes to ions (*2*, *5*). They also increase the permeability of protein-free liposomes (*6*, *7*). The mechanism by which they permeabilize lipid bilayers is not clear, however, although formation of an amphipathic helix appears to be required (*3*). They may form ion channels by inserting into the bilayer and orienting perpendicular to the bilayer with the polar surface of the amphipathic helix facing the interior of the channel. Alternatively, they may permeabilize the bilayer if the amphipathic helix lies on the surface of the bilayer with the hydrophobic surface dipping into the bilayer, thus disturbing the lipid packing.

Electrophysiological studies indicated that magainin formed an ion channel (*4*, *8*−*10*). The kinetics of permeabilization of lipid vesicles induced by magainin is consistent with formation of transient channels followed by translocation of the magainin to the other side of the bilayer (*11*, *12*). Translocation of the peptide across the bilayer is supported by changes in resonance energy transfer from Trp in magainin to a dansylated lipid and by changes in the susceptibility of magainin to digestion by trypsin (*11*). Permeabilization of membranes has been found to be a highly cooperative process, also supporting channel formation (*8*, *11*−*16*). Oriented CD studies showed that at low concentrations, the magainin was oriented parallel to the bilayer, but at higher concentrations, a substantial fraction of the membrane-bound magainin reoriented perpendicular to the plane of the bilayer (*17*). A neutron in-plane scattering technique detected D_2O within the lipid bilayer, suggesting the presence of channels (*18*).

However, a number of studies also support a parallel bilayer orientation. In contrast to oriented CD studies (*18*), solid state NMR studies of oriented peptide−lipid bilayers showed that the peptide was oriented parallel to the bilayer (*19*, *20*). NMR studies of ^{13}C-labeled Ala_{19}-magainin 2 amide in phospholipid bilayers showed that ^{13}C-labeled Ala 15 and Gly 18 were located close to ^{31}P in the lipid headgroups, supporting a parallel bilayer orientation (*21*). In addition, the same study showed that all amide groups of the peptide rapidly exchanged with deuterium in a D_2O atmosphere. Fluorescence quenching studies of a magainin analogue with Trp inserted into the peptide at positions 5, 12, and 16 showed that all three Trps were located at the interface region independent of the lipid:peptide ratio (*13*).

† This work was supported by the Medical Research Council of Canada (J.M.B.). E.J. was supported by a studentship from the Multiple Sclerosis Society of Canada and by an Ontario Graduate Scholarship.

‡ The Hospital for Sick Children and University of Toronto.

§ Ohio University.

* To whom correspondence should be addressed at The Research Institute, The Hospital for Sick Children, Toronto, Canada M5G 1X8. Telephone: (416) 813-5919. Fax: (416) 813-5022. E-mail: jmboggs@sickkids.on.ca.

S0006-2960(98)00855-1 CCC: $15.00
Published on Web 09/11/1998

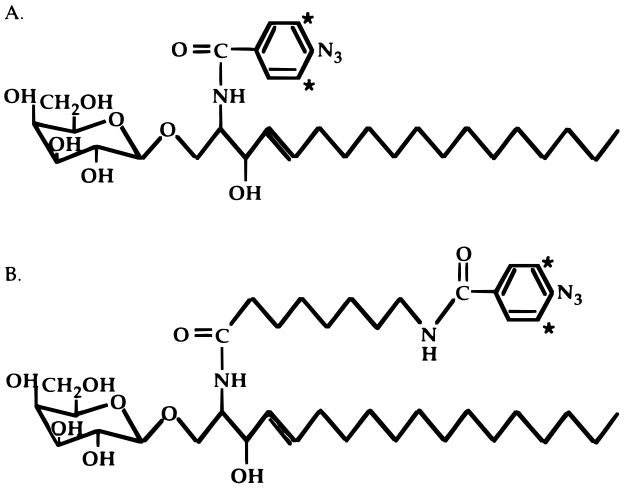

FIGURE 1: Structure of the lipid photolabels used: (A) GalCer-PL and (B) GalCer-C8-PL.

The efficiency of fluorescence energy transfer from Trp_{16}-magainin to dansylmagainin was lower than predicted even for monomeric magainin, not supporting formation of stable oligomers of magainin (*22*).

A toroidal model in which the peptides lining the channel are separated by lipid molecules oriented parallel to the bilayer has been invoked to accommodate some of the above results which seem to be inconsistent with the channel model (*18*, *23*). The toroidal model was supported by the fact that translocation of magainin was accompanied by the flip-flop of fluorescent lipids across the bilayer (*23*) and by the large size of the water channel detected by neutron scattering (*18*). Lytic peptides which permeabilize the bilayer by lying on the surface usually induce negative curvature strain, resulting in a localized disruption of the bilayer structure (*24*, *25*). However, magainin 2 amide must induce a positive curvature strain since it stabilizes the bilayer phase, relative to the hexagonal phase, of phosphatidylethanolamine (PE) (*26*). The induction of positive curvature would facilitate toroidal channel formation. A short lifetime of the channel would also account for the presence of most of the peptide on the bilayer surface and the difficulty in detecting a channel structure formed by only a fraction of the peptide molecules by spectroscopic techniques.

To clarify the mechanism of magainin action, we have used the hydrophobic photolabeling technique (*27*) to detect magainin molecules which are inserted deeply into the bilayer. We used two lipid photolabels (Figure 1) which should position the photosensitive group at two locations in the bilayer, one relatively close to the interface between the apolar and polar regions and the other located near the center of the bilayer. Depth-dependent photolabeling of several proteins, including Sendai virus fusogenic protein, cholera toxin, and cytochrome oxidase, has been achieved using similar "shallow" and "deep" phosphatidylcholine photolabels (*28*−*30*). Ala_{19}-Magainin 2 amide (Ala_{19}-magainin[1]), an analogue of magainin 2 amide in which Ala replaces Glu at position 19 (*31*), and magainin 2 amide (magainin) were used in this study. Ala_{19}-Magainin has significantly greater antimicrobial activity than magainin (*21*). Photolabeling should be able to detect the presence of even a small fraction of the peptide inserted perpendicular to the bilayer, and an increase in insertion with an increase in the peptide:lipid ratio should lead to a significant increase in the extent of labeling. Since the photolabeling reaction is rapid, even peptides which transiently penetrate through the bilayer should still be labeled.

MATERIALS AND METHODS

Lipids and Peptide. Egg L-α-phosphatidylcholine (PC) was purchased from Sigma (St. Louis, MO). L-α-Phosphatidylglycerol (PG) prepared from egg PC and dipalmitoylphosphatidylglycerol (DPPG) were obtained from Avanti Polar Lipids, Inc. (Alabaster, AL). [^{14}C]Dipalmitoylphosphatidylcholine (DPPC) (110 mCi/mmol) was purchased from Dupont-NEN (Boston, MA). Lipid photolabels, [^{3}H]-*N*-4-azidobenzoyl galactosylceramide (GalCer-PL, MW of 605) and [^{3}H]-*N*-(ω-4-azidobenzoylamido) capryloyl galactosylceramide (GalCer-C8-PL, MW of 750) (Figure 1), were synthesized in our laboratory (J. M. Boggs, G. Rangaraj, and K. M. Koshy, unpublished). Briefly, succinimidyl [^{3}H]-azidobenzoate was diluted with cold succinimidyl azidobenzoate to give a specific activity of 0.2−1.2 mCi/μmol (Dupont-NEN, Boston, MA), and it was reacted with psychosine (Sigma) or with ω-amino capryloyl psychosine, synthesized from psychosine. Specific activities of 2×10^5 and 9.5×10^5 cpm/nmol were obtained for [^{3}H]GalCer-PL and [^{3}H]GalCer-C8-PL, respectively. Ala_{19}-Magainin 2 amide and magainin 2 amide were synthesized using Fmoc chemistry and purified by reverse-phase HPLC (*21*).

Preparation of Large Unilamellar Vesicles (LUVs). Aliquots of chloroform solutions of PC and PG were combined to give the desired mole ratio. For vesicles to be used for photolabeling, an appropriate amount of [^{3}H]GalCer-PL or [^{3}H]GalCer-C8-PL in chloroform/methanol (2:1) was added to give 3.3×10^5 cpm/mg of lipid; the lipid:photolabel ratio was kept constant since most of the photolabel reacts with lipid. The lipid photolabels were added in the dark, and the samples were kept in the dark until they were exposed to UV radiation to prevent unwanted photolabeling reaction under light. The organic solvent was evaporated under a stream of nitrogen. To achieve homogeneous mixing of the lipids, the dry lipid film was redissolved in 1−2 mL of benzene, frozen, and lyophilized overnight in the dark.

Multilamellar vesicles (MLVs) were prepared by hydrating the dry lipid in 1 mL of 10 mM phosphate buffer (pH 7.2) containing 150 mM KCl and 0.5 mM EDTA. The concentration of total lipid was 8−24 mg/mL. MLVs were formed by vortexing the suspension for 15 min at room temperature in the dark. The MLVs were freeze-thawed five times using a dry ice/acetone bath and a warm water bath to promote equilibrium transmembrane solute distribution (*32*). Large unilamellar vesicles (LUVs) were prepared with an Avestin LiposoFast extruder (Ottawa, ON) by passing the MLVs through polycarbonate filters with a 400 nm pore size 19 times under manual pressure, followed by 200 nm pore size and then by 100 nm pore size filters, 19 times each (*33*).

[1] Abbreviations: PC, phosphatidylcholine; PG, phosphatidylglycerol; DPPG, dipalmitoylphosphatidylglycerol; DPPC, dipalmitoylphosphatidylcholine; GalCer-PL, [^{3}H]-*N*-(4-azidobenzoyl) galactosylceramide; GalCer-C8-PL, [^{3}H]-*N*-(ω-4-azidobenzoylamido) capryloyl galactosylceramide; MLVs, multilamellar vesicles; LUVs, large unilamellar vesicles; Ala_{19}-magainin, Ala_{19}-magainin 2 amide; magainin, magainin 2 amide.

Ten microliters of vesicle suspension was taken in duplicate before and after extrusion and counted for ^3H to adjust the lipid concentration after extrusion. The LUVs were kept in the dark and were used for addition of peptide and circular dichroism or photolabeling experiments within a few hours.

Circular Dichroism Measurements. Circular dichroism (CD) spectra were recorded on a Jasco-J720 spectropolarimeter at room temperature, using a 1 mm path length quartz cell to minimize the absorbance due to buffer components. Twenty microliters of an Ala_{19}-magainin stock solution in the same buffer (1.9 mg/mL) was added to the LUV suspension (500 μL) or to the same volume of buffer and the mixture equilibrated for 5 min before CD measurements. The final peptide concentration was 30 μM in the absence or presence of LUVs which were composed of egg PC with 0−30 mol % egg PG. The lipid:peptide mole ratio was typically 32:1. Freshly prepared LUVs were used to minimize lipid oxidation. Four scans were averaged for each sample, and averaged background spectra of the buffer or the peptide-free LUVs were subtracted. The ellipticity at 222 nm was used to calculate the relative helicity. According to $[\theta]_{222nm} = -39500(1 - 2.75/n)$ where n is the number of amino acids in the peptide, a $[\theta]_{222nm}$ of -34777 deg cm^2 dmol^{-1} was taken as the value for 100% α-helix of a 23-amino acid peptide (*34*).

Photolabeling Reaction. For the samples with a lipid:peptide mole ratio of 32:1, 60 μg of Ala_{19}-magainin or magainin from stock solutions (1 mg/mL) was added to LUVs (100% PC or 20% PG/80% PC) diluted to contain 0.6 mg of lipids in 600 μL of 10 mM phosphate buffer (pH 7.2) containing 150 mM KCl and 0.5 mM EDTA. For lipid:peptide mole ratios of 96:1 and 160:1, 60 μg of Ala_{19}-magainin was added to LUVs containing 1.8 and 3.0 mg of lipid in 600 μL, respectively. Thus, the amount of peptide per sample was kept constant. The sample was mixed by gentle shaking and equilibrated in the dark at room temperature for 5 min. For the kinetic study, the time for equilibrium was varied from 0 to 30 min. The sample was then irradiated for 30 s, with the sample tube immersed in ice/water, using a 100 W high-pressure Hg lamp (Photochemical Research Associates, London, ON). The light beam was cooled by passage through a reservoir of circulating cold water and was directed through a filter (Oriel Corp., Stratford, CT) which cuts off the light at short wavelengths below 235 nm.

To determine the ability of these probes to label a water soluble protein, myelin basic protein (MBP) was used with the probes incorporated in PC vesicles. MBP does not bind to pure PC vesicles (*50*). The most positively charged component, C1, of bovine brain MBP was used, purified as described earlier (*51*). MLVs of PC containing lipid photolabels (2.8×10^6 cpm/mg of lipid, 0.53 mg of PC/mL) were prepared in 10 mM Hepes buffer containing 10 mM NaCl and 1 mM EDTA at pH 7.4 as described above. A MBP solution (2 mg/mL) in 10 mM Hepes buffer containing 10 mM NaCl and 1 mM EDTA at pH 7.4 was prepared. A 30 μL aliquot containg 60 μg of MBP was added to 0.25 mg of PC in 470 μL of buffer, and the MLVs were dispersed again by vortexing. The sample was equilibrated in the dark at room temperature for 20 min and then irradiated for 30 s as described for magainin peptides.

The azidobenzoyl photolabels are activated at 270 nm and generate nitrenes. Although aryl azides are sensitized and react rapidly, they have a finite lifetime. The half-life for photosensitization of the arylazide used here has been reported as 30-60 s (*35*). Thus, it is likely that the photolabels continue to generate nitrenes which continue to react over the 30 s irradiation time. This short irradiation time was found to cause no degradation of the larger protein MBP or of magainin peptides under these conditions. Photolabels can also react with lipid which can then bind noncovalently to the peptide by electrostatic interactions. To determine the amount of labeled lipid remaining noncovalently bound to the peptide after purification procedures, a control sample of LUVs without peptide or MLVs without MBP was also photolabeled. Then, unlabeled peptide or MBP was added to the photosensitized lipids, using the same procedure that was used when adding it to lipid before photosensitization. The control samples as well as the other samples were treated identically by the purification steps described below.

Purification of the Photolabeled Peptide. Magainin did not run properly on gels in the presence of lipid and also could not be separated from the labeled lipid by gel electrophoresis. Therefore, a Microcon-SCX microconcentrator (Amicon Canada Ltd.) with a cation exchange membrane was used to purify the cationic magainin peptides from the peptide/lipid mixture. To remove lipid from peptide and recover the labeled peptide, the following procedure was developed. To wet the membrane of the Microcon-SCX instrument, 200 μL of methanol was added to the device and it was centrifuged at 1200*g* (model GS-15R centrifuge, Beckman) for 1 min. This was repeated twice with 200 μL of double-distilled water. To 600 μL of lipid/peptide samples were added 60 μL of Triton X-100 (10%, v/v) (Sigma) and 540 μL of double-distilled water, since samples must contain <100 mM salt to prevent saturation of the cation exchange membrane with cations. The samples were vortexed vigorously, and an aliquot (400 μL) was loaded into the Microcon-SCX instrument for binding of the peptide. The device was centrifuged at 1200*g* for 1 min, and this was repeated twice with the rest of the sample (2×400 μL) for accumulative binding of the peptide from the entire sample onto one Microcon-SCX unit. For the highest sample recovery, the device orientation in a fixed-angle rotor was kept constant for each subsequent centrifugation. To remove residual lipids, three wash steps were conducted, first using double-distilled water, followed by 50% methanol, followed by 50% acetonitrile (500 μL each), respectively. In preliminary trials with liposomes containing [^{14}C]DPPC, this procedure eluted over 99% of the radioactive lipid.

For peptide elution, 75 μL of the desorption reagent (7 N NH_4OH in 50% acetonitrile) was then placed into the Microcon-SCX instrument containing the bound peptide. It was centrifuged at 14000*g* for 1 min, and the elution step was repeated twice with fresh desorption reagent (2×75 μL) to maximize yields. NH_4OH (7 N) was found to be necessary to elute most of the peptide. Higher concentrations failed to elute more peptide. The final eluted sample was lyophilized using a Speed Vacuum Concentrator (Savant) to remove ammonium and acetonitrile. To the dry samples were added 30 μL of commercial NOVEX (2×) sample buffer [3 M Tris-HCl (pH 8.45) containing glycerol (0.24

FIGURE 2: SDS gel of the photolabeled Ala_{19}-magainin after purification from lipid: lane 1, approximately 5 μg of the photolabeled peptide eluted from the Microcon-SCX microconcentrator; and lane 2, 5.0 μg of unlabeled peptide from a standard solution. Peptides were loaded on a 16% Tricine gel and stained with Coomassie Blue. Arrowheads at the top and bottom indicate the top and bottom of the gel, respectively.

mg/mL), SDS (80 μg/mL), 0.1% Coomassie Blue G, and 0.1% Phenol Red, with 5% β-mercaptoethanol] and 30 μL of double distilled water, and the sample was vortexed for further analysis by SDS−PAGE. Aliquots of the Microcon-SCX flow-through (50 μL), the washes (50 μL), and the final eluted samples in sample buffer (5 μL) were taken, and 6 mL of scintillation cocktail (Ready Safe, Beckman) was added. The ^{3}H radioactivity was counted in a β counter (Beckman LS 6000IC).

SDS−Polyacrylamide Gel Electrophoresis. An aliquot of the peptide in sample buffer expected to contain about 5 μg of the purified peptide and an aliquot of a standard Ala_{19}-magainin or magainin solution containing 5.0 μg of peptide were loaded on 16% Tricine gels (NOVEX). Electrophoresis was performed at 100 V (constant voltage) until the tracking dye reached the bottom of the gel. A typical SDS−PAGE gel of the eluted photolabeled Ala_{19}-magainin is shown in Figure 2. After the gel was stained with 0.05% Coomassie Brilliant Blue R and destained as described (*36*), the gel was scanned in a gel scanner (White/UV Transilluminator, DiaMed Lab Supplies Inc.). The band intensity was integrated using UVP Grab-It software. The peptide was quantitated by comparing its band intensity with that of the standard band (5 μg) which fell in the linear range of a standard curve. For elution of the radioactive peptide from the gel, each lane was sliced into six strips and each strip placed into scintillation vials in small pieces. A gel oxidizing solution was freshly made from 19 parts of 30% H_2O_2 and 1 part of 14.8 M NH_4OH (*37*). Nine hundred microliters of the oxidizing solution was added into each scintillation vial, and it was incubated at 37 °C overnight. For efficient radioactivity counting, the alkalinity of the oxidizing solution was then neutralized by adding 100 μL of glacial acetic acid. Finally, 6 mL of scintillation cocktail was added, and the ^{3}H radioactivity was counted in a β counter. Counts in gel strips above and below the peptide band were at background levels. In addition, control samples, in which the peptide was added to the labeled vesicles after irradiation, had low counts in the gel slice containing the peptide, indicating that all noncovalently bound lipids were removed by the Microcon-SCX microconcentrator and SDS−PAGE. Specific activities were obtained (counts per minute per microgram) and were divided by the original radioactivity available per microgram of peptide and multiplied by 100 to give percentage labeling values (percentage of the added photolabel bound to peptide).

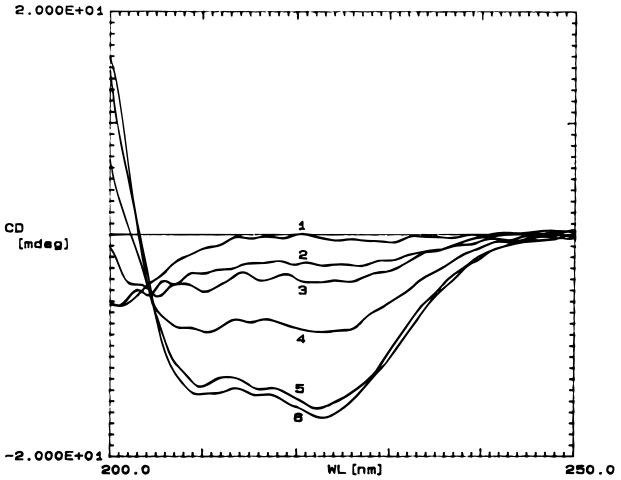

FIGURE 3: CD spectra of Ala_{19}-magainin: Ala_{19}-magainin in aqueous buffer (1) and in the presence of PC vesicles with 0, 5, 10, 20, and 30% PG (curves 2−6, respectively). The peptide concentration was 30 μM, and the lipid:peptide molar ratio was 32:1. Each spectrum was the average of four scans with the background of the buffer (1) or the vesicles (2−6) subtracted.

Determination of the Amount of Photolabel Bound to MBP. Since the presence of lipid did not affect the way MBP ran on gels and since MBP did not run as far as the labeled lipid on the gels, we were able to separate the MBP from labeled lipid by gel electrophoresis without extraction of the lipid. Photolabeled samples were lyophilized and resuspended in 120 μL of H_2O. To a 35 μL aliquot was added 35 μL of sample buffer (2×). Twenty microliters of the MBP samples in sample buffer containing 5 μg of MBP was loaded onto each of three adjacent lanes on 16% Tricine gels. Electrophoresis and staining were carried out as described above. MBP gels were sliced into 14 strips, keeping the three adjacent lanes loaded with the same sample together. Each strip of three lanes was counted as described above. Labeled lipid appeared in strips well below the MBP band.

RESULTS

Secondary Structure of Ala_{19}-Magainin. Ala_{19}-Magainin has a random structure in aqueous solution (Figure 3). In the presence of lipid vesicles, the extent of α-helicity

Table 1: Estimated α-Helical Contents of Ala_{19}-Magainin[a]

	α-helical content (%)		α-helical content (%)
aqueous buffer	0.7	10% PG	36
PC	11	20% PG	65
5% PG	18	30% PG	68

[a] The ellipticity at 222 nm in CD spectra was used to calculate the relative helicity where a $[\theta]_{222nm}$ of −34777 deg cm^2 dmol^{-1} was taken as the value for 100% α-helix of a 23-amino acid peptide (*34*).

increased as the content of acidic lipid increased from 5 to 20% PG (Figure 3 and Table 1). At a lipid:peptide mole ratio of 32:1, for vesicles containing ∼20% PG, where the number of positive charges on Ala_{19}-magainin is equal to the number of negative charges on PG, the maximal extent of binding occurred and the α-helicity reached a plateau at 65−68%. Both the N-terminal α-amino group and the His 7 residue are assumed to be protonated since the local pH of the acidic membrane surface is lower than that of the bulk solution (pH 7.2); thus, this peptide has six positive charges. The spectra of the peptide in the presence of vesicles containing 20% PG and 30% PG are those of the completely membrane-bound form because further addition of vesicles did not cause any further change in the spectrum (not shown). The percentage of α-helicity found for vesicles containing 20−30% PG is similar to that found for Ala_{19}-magainin bound to 1:1 DPPC/DPPG vesicles by Hirsh et al. (*21*) using FTIR and NMR spectroscopy.

The CD spectrum of Ala_{19}-magainin in the presence of 100% PC (the spectrum for lipid itself subtracted) showed some α-helical content but less than in the presence of vesicles containing 5% PG (Table 1). The anionic phosphate group of PC may bind some Ala_{19}-magainin, resulting in the formation of α-helices in a small population. Matsuzaki et al. (*6*) and Duclohier et al. (*10*) detected a small increase in the extent of helicity of magainin 1 also upon addition of egg PC SUVs, using CD measurements. In addition, Raman spectroscopy estimated the secondary structure of magainin 2 to be 35−47% α-helical at DPPC:peptide mole ratios from 4:1 to 59:1 at both 14 and 50 °C in the gel and liquid crystalline phases, respectively (*38*). This group also found that magainin 2 caused vesiculation of zwitterionic PC MLVs into smaller particles at lipid:peptide mole ratios below 4:1.

Photolabeling of Ala_{19}-Magainin and Magainin in Lipid Bilayers. Hydrophobic photolabeling was performed to determine whether Ala_{19}-magainin inserts into the lipid bilayer. These lipid photolabels incorporated into PC vesicles did not label a water soluble protein, myelin basic protein, a protein which does not bind to PC, indicating that they do not label from the aqueous phase. Only 0.07% of the added GalCer-PL and 0.1% of the GalCer-C8-PL reacted with MBP in solution in the presence of PC vesicles, when the protein was 19.4 wt % of the sample. In contrast, 15% of the GalCer-PL reacted with Ala_{19}-magainin when bound to acidic lipid vesicles containing 20% PG at a lipid:peptide (L:P) mole ratio of 32:1 (which is 9.4% of the mass of the vesicles at this ratio). Only 0.5−0.9% of the probe was found to be associated with the peptide for control samples in which the peptide was added to the vesicles after irradiation. Since Ala_{19}-magainin binds much more to PC/PG than to PC vesicles, it should be labeled more in the presence of PC/PG vesicles than in the presence of PC vesicles. Indeed, at a L:P mole ratio of 32:1, Ala_{19}-magainin was labeled 2.4 times more by GalCer-PL when bound to 4:1 PC/PG vesicles than PC vesicles (Figure 4). This extent of labeling suggests that following electrostatic interaction of Ala_{19}-magainin with acidic lipids, it subsequently interacts hydrophobically with the lipid bilayer.

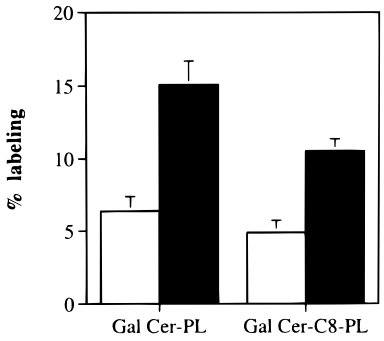

FIGURE 4: Percentage of the photolabel bound to Ala_{19}-magainin in PC LUVs (white bars) or 4:1 PC/PG LUVs (black bars) by GalCer-PL and GalCer-C8-PL. The extent of hydrophobic photolabeling of Ala_{19}-magainin by GalCer-PL was compared with that by GalCer-C8-PL. The lipid:peptide mole ratio was 32:1. Data presented for GalCer-PL are the average of five sets of gels from duplicate samples. Data presented for GalCer-C8-PL are the average of five sets of gels from two photolabeling experiments for PC and eleven sets of gels from four photolabeling experiments for 4:1 PC/PG. The mean ± standard deviation is shown.

However, the shallow GalCer-PL might label the peptide when it is bound on the surface of the bilayer. Therefore, the deeper GalCer-C8-PL was also used. Its photoreactive group should be accessible to peptide groups near the center of the bilayer, and it is likely to label the peptide more when it is inserted deeply into the bilayer than when it is on the surface. The extent of labeling by GalCer-C8-PL for vesicles containing 20% PG ranged from 70 to 117% of that by GalCer-PL, suggesting that Ala_{19}-magainin inserts deeply into the lipid bilayer at least transiently (Figure 4; also see Figure 7). GalCer-C8-PL labeled the peptide 2.2 times more when bound to acidic lipid vesicles containing 20% PG than PC vesicles (Figure 4).

Peptide Concentration-Dependent Photolabeling. The extent of labeling should depend on the L:P ratio if the peptide forms channels since this is a highly cooperative process (*8*, *11*−*16*). Therefore, the dependence of the extent of labeling on the L:P ratio was determined. A fixed concentration of the peptide was mixed with various amounts of 20% PG LUVs to vary the lipid:peptide ratio, and the extent of photolabeling was examined. Using oriented circular dichroism (OCD), Ludtke et al. (*17*) has shown that a substantial fraction of the membrane-bound magainin reorients itself perpendicular to the plane of the lipid bilayer at a critical concentration (a L:P molar ratio of ∼30:1) in the presence of DMPC/DMPG (3:1) multilayers. Although the critical concentration may depend on the lipid composition of the membranes (*18*), we have chosen to use the molar ratios 32:1, 96:1, and 160:1 for investigation of the dependence of the extent of labeling on peptide concentration.

Although there was a greater extent of photolabeling of Ala_{19}-magainin by GalCer-PL in the presence of vesicles containing 20% PG than PC vesicles at a L:P mole ratio of 32:1, the presence of 20% PG did not enhance the extent of photolabeling at a L:P ratio of 160:1 (Figure 5A). At a L:P

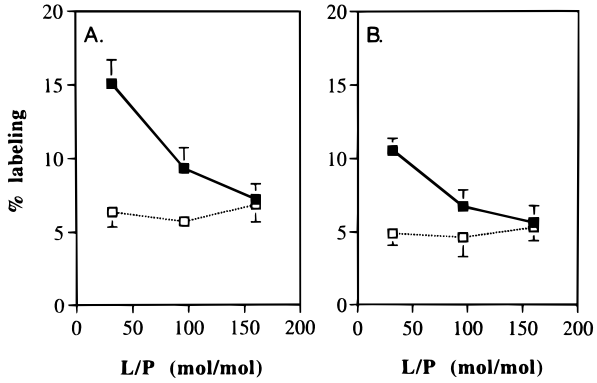

FIGURE 5: Peptide concentration-dependent extent of photolabeling by (A) GalCer-PL and (B) GalCer-C8-PL of Ala_{19}-magainin in PC LUVs (□) or PC LUVs containing 20% PG (■). The percentage of the photolabel bound to peptide is shown. Data presented for GalCer-PL are the average of five sets of gels from duplicate samples. Data presented for GalCer-C8-PL are the average of five sets of gels from two photolabeling experiments for PC and eleven sets of gels from four photolabeling experiments for 20% PG. The mean ± standard deviation is shown.

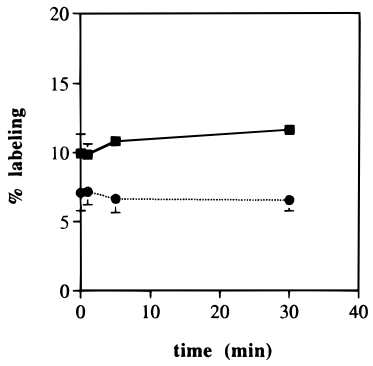

FIGURE 6: Insertion occurs rapidly after addition of Ala_{19}-magainin to membranes. At different time points after addition of Ala_{19}-magainin to 20% PG LUVs containing GalCer-C8-PL, an aliquot of the sample was irradiated. The L:P mole ratio was 32:1 (■) and 96:1 (●). Data presented are the average of six sets of gels from duplicate samples. The mean ± standard deviation is shown.

ratio of 96:1, the extent of photolabeling was between the above two ratios. Thus, the extent of labeling in the presence of vesicles containing 20% PG increased with an increase in the peptide:lipid ratio. Figure 5B shows a similar dependence of the extent of labeling by GalCer-C8-PL on the L:P ratio. This greater extent of labeling at lower L:P ratios occurred although the amount of probe:peptide ratio was lower at lower L:P ratios (since the probe:lipid ratio was kept constant). Thus, the accessibility of magainin to the photolabels in the bilayer is a cooperative process as found for the permeabilization of membranes by magainin.

Kinetic Study. To examine the kinetics of bilayer insertion, we photolabeled aliquots of the sample at different time points. The extent of hydrophobic photolabeling was similar from 0 to 30 min after adding Ala_{19}-magainin to the lipid vesicles at a L:P ratio of either 32:1 or 96:1 (Figure 6). This suggests that the peptide insertion takes less than 30 s which is the time consumed for UV irradiation. The results reveal further that the peptide remains inserted for 30 min or, alternatively, that it has achieved an equilibrium state between inserted and noninserted peptide by 30 s.

Comparison of the Extents of Labeling of Ala_{19}-Magainin and Magainin. Reactivity of the photolabels with Ala_{19}-magainin and magainin bound to vesicles containing 20% PG was compared at a L:P ratio of 32:1. In this experiment, both photolabels labeled the peptide similarly. There was no significant difference in the extent of labeling of Ala_{19}-magainin and magainin by either photolabel (Figure 7). Thus, both peptides are able to insert to a similar degree into the bilayer at this L:P ratio.

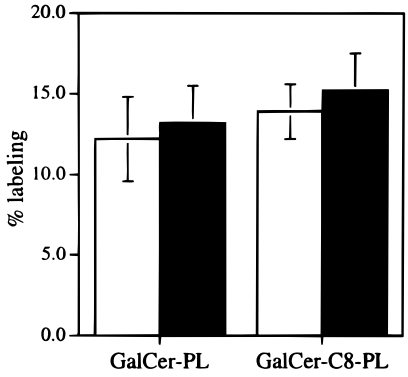

FIGURE 7: Percentage of the photolabel bound to Ala_{19}-magainin (white bars) and magainin (black bars) in 4:1 PC/PG LUVs by GalCer-PL and GalCer-C8-PL. The lipid:peptide mole ratio was 32:1. Data are the average of three sets of gels from one photolabeling experiment. The mean ± standard deviation is shown.

DISCUSSION

Lipid photolabels which should position the photolabel group at different depths within the bilayer were used to determine whether magainin inserts deeply into the bilayer. Although a similar phospholipid photolabel with the photolabel group at the end of a C11 acyl chain was found to cross-link adjacent phospholipid molecules maximally at carbon 12 (*39*), it cannot be concluded that lipid photolabels achieve depth-dependent labeling with 100% confidence. The lipid chain may flip up to the surface of the bilayer and label peptide residues at the surface. Photolabels are much more reactive with nucleophilic groups than CH groups, and may even preferentially label more reactive amino acids such as Trp at the bilayer surface than hydrophobic ones deeper in the bilayer (*40*). However, magainin has a number of reactive amino acids, including three Phes, throughout its sequence, and should react well with a photolabel at the end of an acyl chain, if the peptide is inserted perpendicular to the bilayer.

A phospholipid photolabel carrying an aromatic carbene precursor at the end of an eleven-carbon chain appeared to achieve depth-dependent photolabeling of alamethicin in lipid bilayers (*41*). Although alamethicin is more hydrophobic than magainin, it is thought to form transient, concentration-dependent ion channels (*42*, *43*). Consistent with an orientation of alamethicin perpendicular to the bilayer, this peptide reacted with the photolabel only at its N-terminal half, suggesting that the lipid chain did not flip up to the bilayer surface to label all residues.

In a study of the membrane topology of the Sendai virus fusogenic protein (*28*), a phosphatidylcholine photolabel with an aryl azide at the end of a C12 chain did not label a domain which was labeled by a lipid photolabel with the aryl azide linked directly to the glycerol backbone. However, it did label a more hydrophobic region containing a putative transmembrane domain almost as well as the shallow probe.

Thus, the photolabel positioned at the end of an acyl chain was able to discriminate between a peptide on the bilayer surface containing the fusion peptide and one inserted into the hydrophobic core. These shallow and deep photolabels also showed depth-dependent extents of labeling of the α, *β*, and *γ* subunits of cholera toxin (*29*) and of subunits of cytochrome oxidase (*30*).

Lipids with fatty acids carrying a nitroxide group or a bromine at different positions along the fatty acid chain are used to monitor the depth of Trp in proteins and peptides through their ability to quench Trp fluorescence. Although as for aryl azide groups, the nitroxide group is considerably bulkier and more polar than Br, nitroxide-labeled lipid chains have been found to result in depth-dependent quenching similar to that of brominated lipid chains, indicating that the nitroxide groups reside close to their predicted locations in the bilayer (*44*). Such spin-labeled lipids were used to monitor the location of Trp 5, 12, and 16 in Trp-substituted magainin analogues. All three Trps were found at a depth of 8−10 Å from the bilayer center, between carbons 5 and 10 of the acyl chain, indicating that the major peptide population is oriented parallel to the bilayer (*13*). Of particular relevance to this work, that study showed that a deep nitroxide probe did not quench Trp on the surface as much as more shallow nitroxides, thus indicating that these probes remained near their expected locations even in the presence of magainin.

In view of the ability of these probes to achieve depth-dependent labeling and considering that magainin has reactive groups all along its sequence, the labeling of Ala_{19}-magainin and magainin by both the shallow and deep lipid photolabels suggests that a significant proportion of the bound peptide inserts deeply into the bilayer, at least transiently. Although the acyl chain of GalCer-C8-PL might be able to also label peptide on the surface to some extent, its extent of labeling of surface-bound peptide should be much less than that of inserted peptide.

Although the peptides appear to insert deeply, this does not necessarily mean that they insert in a perpendicular orientation in a transmembrane fashion. A model of the amphipathic helix of Ala_{19}-magainin is shown in Figure 8. The replacement of Glu_{19} in magainin 2 with Ala makes Ala_{19}-magainin less amphipathic at the C-terminal end and gives this end a more overall hydrophobic character. Peptides with an asymmetric amphipathic structure tend to be fusogenic and probably also lytic (*45*). Such peptides may insert obliquely into one-half of the bilayer as suggested by Brasseur (*45*), thus disturbing lipid packing. The high degree of photolabeling of the magainin peptides could be consistent with either a transmembrane orientation or, in the case of Ala_{19}-magainin, an oblique insertion into half of the bilayer.

The degree of labeling of Ala_{19}-magainin by both photolabels increased with peptide:lipid ratio in the acidic vesicles. This supports a model of channel formation by peptides with a transmembrane orientation. The concentration dependence of peptide interaction with the lipid could indicate peptide aggregation in the bilayer according to a theoretical model (*46*). The probability of forming an oligomeric structure such as a channel (either a regular channel or a toroidal channel) is greater at higher peptide:lipid ratios. Formation of a channel would lower the energy state of the peptide when it is inserted into the bilayer because the polar surface of the amphipathic helix can face the center of the channel away from the hydrophobic lipid chains.

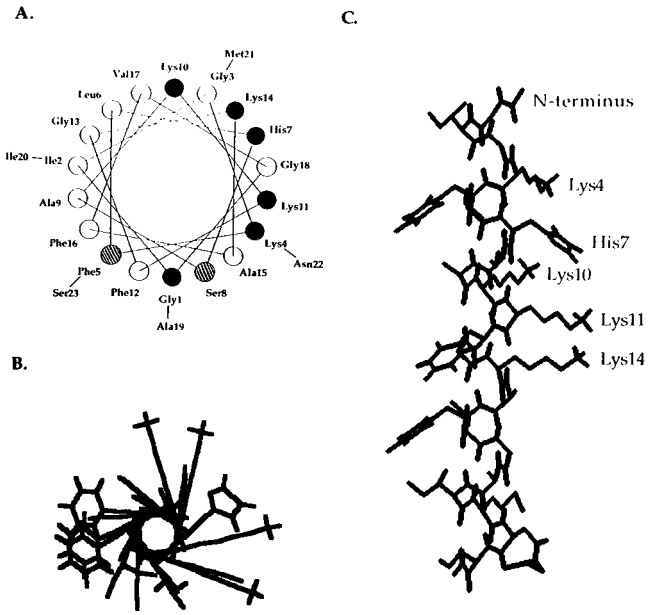

FIGURE 8: Model of the amphipathic α-helical structure of Ala_{19}-magainin. (A) A helical wheel diagram. Positively charged residues, including N-terminal Gly 1, are shown as filled circles, and polar residues are shown as hatched circles. Hydrophobic residues and Gly are shown as open circles. (B) A molecular model (top view) of helical Ala_{19}-magainin constructed using the Rasmol program. Positions of amino acid residues are the same as in panel A. (C) A molecular model (side view) of helical Ala_{19}-magainin. Only the N-terminal half of the peptide is amphipathic, while the C-terminal half is neutral or hydrophobic on both faces of the helix, in contrast to magainins 1 and 2.

A significant increase in the extent of labeling occurred at a L:P ratio of 32:1. The L:P ratio at which an increased extent of labeling occurs correlates with a change in orientation of the peptide with respect to the bilayer plane from parallel to perpendicular, observed by Ludtke et al. (*17*), and a change in the enthalpy of interaction of the peptide with lipid from exothermic to endothermic, observed by Wenk and Seelig (*49*). The observed extent of labeling at low peptide concentrations (L:P ratio of 160:1) in vesicles containing 20% PG, which is similar to that in the presence of PC vesicles, may be due mainly to surface binding of the peptide. Even if more peptide is bound to the 20% PG vesicles at any given time, there is undoubtedly fast exchange between free and bound peptides, especially for the PC vesicles, which could account for a similar extent of labeling for PC vesicles and vesicles containing 20% PG at low peptide concentrations. Once a peptide is photolabeled, it is probably trapped on the vesicle and can no longer dissociate. Over time (i.e., during the 30 s illumination period), a large sampling of the total peptide population is probably available for labeling in the PC vesicles. As the concentration of the surface-bound peptide increases at lower L:P ratios for 20% PG vesicles, leading to cooperative insertion and channel formation, an increased extent of labeling above the baseline level is observed.

It could be argued that the greater extent of labeling at higher P:L ratios is a result of a greater extent of labeling of peptide which remains surface-bound, as a consequence of greater disordering of the bilayer and more flipping up of

the acyl chain of GalCer-C8-PL. However, this should result in an increase in the ratio of labeling by GalCer-C8-PL relative to that by GalCer-PL. This does not occur; the ratio of labeling by both probes remains relatively constant at all L:P ratios. The extent of labeling by the more shallow probe also increases with L:P ratio. It may also be able to label inserted peptide more readily than surface-bound peptide.

Many investigators have suggested that the lifetime of the magainin channel is very short and the population of magainin forming channels is too small to be detected by many methods, such as spectroscopic techniques. Use of the hydrophobic photolabeling technique to study the mode of interaction of magainin with membranes can overcome the low sensitivity of other techniques in detecting channels. If magainin peptides insert into the bilayer to form channels at any time during the 30 s of UV irradiation, they become photolabeled in the bilayer. Even if they return to the membrane surface, the photolabel is still bound to the peptide. Therefore, the hydrophobic photolabeling technique can detect the occurrence of more channels than the number of channels actually present at one time point.

The extent of labeling of the peptide was greater than expected on a mass basis, assuming equal reactivity of the photolabels toward both lipids and peptides. The percentage of the labels bound to magainin at a L:P weight ratio of 10:1 was 10−15% in vesicles containing 20% PG and 5−7% for PC vesicles. On a mass basis, if all of the peptide is available for labeling and if the photolabel reacts equally with lipid and peptide, the amount of label associated with peptide should be at most 9.4%. In fact, the extent of labeling of saturated lipids and insertion into C−H bonds by nitrenes is much less than 100% (*40*). A similar high degree of labeling was found for gramicidin and was attributed to the much greater reactivity with Trp relative to insertion into C−H bonds (*40*). In the case of magainin, the high degree of labeling may be due to the presence of three Phes and other nucleophilic groups such as serine hydroxyls in the sequence. Exchange between surface-bound and inserted peptide during the 30 s labeling period may also contribute to the higher degree of labeling in 20% PG vesicles, since the fraction of inserted peptide at any one time point is probably low, especially at high L:P ratios.

Our kinetic study revealed that peptide insertion or channel formation takes less than 30 s and that channels either are stable for at least 30 min for Ala_{19}-magainin or have reached an equilibrium state by 30 s. Magainin causes an initial very rapid phase of leakage of lipid vesicles, followed by a slower phase (*7*, *11*, *12*, *38*). The rapid phase is complete within less than 1 min even at high L:P ratios. Translocation of the peptide follows similar kinetics, leading to the conclusion that the initial rapid phase is due to a high concentration of pores driven by the initial concentration gradient of magainin on one side of the bilayer (*11*, *12*). The pore concentration falls as the peptide translocates to the other side and equilibration of the peptide on both sides of the bilayer occurs. The slower phase of leakage is attributed to back translocation and transient formation of pores at a lower pore density. Matsuzaki et al. (*47*) found that Gln_{19}-magainin 2 amide, which has the same charge distribution as Ala_{19}-magainin 2 amide, translocated to the inner leaflet of the bilayer fastest, within 1 min, and formed the least stable channels compared to several less positively charged analogues. If Ala_{19}-magainin 2 amide behaves like Gln_{19}-magainin 2 amide, the results of our kinetic study probably can be ascribed to an equilibrium state achieved by 30 s, where there is rapid exchange between a small population of the inserted peptide and a larger population of the peptide on the bilayer surface on both sides of the bilayer. If we had been able to achieve more rapid irradiation, a higher degree of photolabeling might have occurred within the first 30 s after peptide addition when the pore density is presumably at its highest.

An ion channel formed by magainin is predicted to be energetically relatively unstable (*48*). Upon channel formation of magainins, the many positively charged residues would come into close contact and repel one another. Therefore, the electrostatic repulsive energy has been estimated to be very high for magainin 2 (*48*). It will be even higher for Ala_{19}-magainin in which Glu_{19} is replaced by Ala since there is no possibility of a salt bridge between peptide monomers. The dipolar repulsion between parallel helical dipoles and the loss in entropy during aggregation also contribute unfavorable energy terms. However, the electrostatic repulsion would be reduced by involvement of negatively charged lipids in the channels, as in the toroidal model (*18*, *23*), or by the presence of salt.

In the toroidal model, magainin remains associated with lipid polar headgroups even though the peptide is inserted perpendicular to the bilayer. This model does not preclude labeling by the lipid photolabels, however, as there are likely some bilayer lipids, whose acyl chains are oriented parallel to the peptide, mixed with the lipids whose headgroups are associated with the peptide. Some of these bilayer lipids likely contact the peptide through their acyl chains. Furthermore, the peptides in such toroidal pores might be more susceptible to labeling since the lipid packing in the region of the pores is disturbed and more of the peptide surface may be exposed to the lipid acyl chains. Thus, although our results cannot confirm the existence of the toroidal model, they also do not rule it out.

In summary, the peptide concentration dependence of the extent of labeling supports peptide insertion and channel formation by both magainin and Ala_{19}-magainin in 20% PG vesicles at a lipid:peptide ratio of 32:1.

ACKNOWLEDGMENT

We thank Dr. C. Yip (University of Toronto, Toronto, ON) for allowing us to use his photolysis equipment, Dr. Li-Ping Liu for help with the CD spectrometer, Ms. Chen Wang for constructing the peptide model, and Dr. K. M. Koshy for synthesizing the lipid photolabels. We are grateful to Dr. W. Lee Maloy (Magainin Pharmaceuticals, Inc.) for providing the peptides.

REFERENCES

1. Giovannini, M. G., Poulter, L., Gibson, B. W., and Williams, D. H. (1987) *Biochem. J. 243*, 113−120.
2. Zasloff, M., Martin, B., and Chen, H.-C. (1988) *Proc. Natl. Acad. Sci. U.S.A. 85*, 910−913.
3. Chen, H.-C., Brown, J. H., Morell, J. L., and Huang, C. M. (1988) *FEBS Lett. 236*, 462−466.
4. Cruciani, R. A., Barker, J. L., Zasloff, M., Chen, H.-C., and Colamonici, O. (1991) *Proc. Natl. Acad. Sci. U.S.A. 88*, 3792−3796.

5. Baker, M. A., Maloy, W. L., Zasloff, M., and Jacob, L. S. (1993) *Cancer Res. 53*, 3052−3057.
6. Matsuzaki, K., Harada, M., Handa, T., Funakoshi, S., Fujii, N., Yajima, H., and Miyajima, K. (1989) *Biochim. Biophys. Acta 981*, 130−134.
7. Grant, E., Jr., Beeler, T. J., Taylor, K. M. P., Gable, K., and Roseman, M. A. (1992) *Biochemistry 31*, 9912−9918.
8. Cruciani, R. A., Barker, J. L., Durell, S. R., Raghunathan, G., Guy, H. R., Zasloff, M., and Stanley, E. F. (1992) *Eur. J. Pharmacol. 226*, 287−296.
9. Haimovich, B., and Tanaka, J. C. (1995) *Biochim. Biophys. Acta 1240*, 149−158.
10. Duclohier, H., Molle, G., and Spach, G. (1989) *Biophys. J. 56*, 1017−1021.
11. Matsuzaki, K., Murase, O., Fujii, N., and Miyajima, K. (1995) *Biochemistry 34*, 6521−6526.
12. Matsuzaki, K., Murase, O., and Miyajima, K. (1995) *Biochemistry 34*, 12553−12559.
13. Matsuzaki, K., Murase, O., Tokuda, H., Funakoshi, S., Fujii, N., and Miyajima, K. (1994) *Biochemistry 33*, 3342−3349.
14. Juretic, D., Hendler, R. W., Kamp, F., Caughey, W. S., Zasloff, M., and Westerhoff, H. V. (1994) *Biochemistry 33*, 4562−4570.
15. Westerhoff, H. V., Juretic, D., Hendler, R. W., and Zasloff, M. (1989) *Proc. Natl. Acad. Sci. U.S.A. 86*, 6597−6601.
16. Westerhoff, H. V., Hendler, R. W., Zasloff, M., and Juretic, D. (1989) *Biochim. Biophys. Acta 975*, 361−369.
17. Ludtke, S. J., He, K., Wu, Y., and Huang, H. W. (1994) *Biochim. Biophys. Acta 1190*, 181−184.
18. Ludtke, S. J., He, K., Heller, W. T., Harroun, T. A., Yang, L., and Huang, H. W. (1996) *Biochemistry 35*, 13723−13728.
19. Bechinger, B., Zasloff, M., and Opella, S. J. (1992) *Biophys. J. 62*, 12−14.
20. Bechinger, B., Zasloff, M., and Opella, S. J. (1993) *Protein Sci. 2*, 2077−2084.
21. Hirsh, D. J., Hammer, J., Maloy, W. L., Blazyk, J., and Schaefer, J. (1996) *Biochemistry 35*, 12733−12741.
22. Schümann, M., Dathe, M., Wieprecht, T., Beyermann, M., and Bienert, M. (1997) *Biochemistry 36*, 4345−4351.
23. Matsuzaki, K., Murase, O., Fujii, N., and Miyajima, K. (1996) *Biochemistry 35*, 11361−11368.
24. Tytler, E. M., Segrest, J. P., Epand, R. M., Nie, S. Q., Epand, R. F., Mishra, V. K., Venkatachalapathi, Y. V., and Anantharamaiah, G. M. (1993) *J. Biol. Chem. 268*, 22112−22118.
25. Epand, R. M., Shai, Y., Segrest, J. P., and Anantharamaiah, G. M. (1995) *Biopolymers 37*, 319−338.
26. Wieprecht, T., Dathe, M., Epand, R. M., Beyermann, M., Krause, E., Maloy, W. L., MacDonald, D. L., and Biener, M. (1997) *Biochemistry 36*, 12869−12880.
27. Brunner, J., and Semenza, G. (1981) *Biochemistry 20*, 7174−7182.
28. Moscufo, N., Gallina, A., Schiavo, G., Montecucco, C., and Tomasi, M. (1987) *J. Biol. Chem. 262*, 11490−11496.
29. Tomasi, M., and Montecucco, C. (1981) *J. Biol. Chem. 256*, 11177−11181.
30. Bisson, R., Montecucco, C., Gutweniger, H., and Azzi, A. (1979) *J. Biol. Chem. 254*, 9962−9965.
31. Cuervo, J. H., Rodriguez, B., and Houghten, R. A. (1990) in *Peptides: Chemistry and Biology* (Rivier, J. E., and Marshall, G. R., Eds.) pp 124−126, ESCOM, Leiden, The Netherlands.
32. Mayer, L. D., Hope, M. J., Cullis, P. R., and Janoff, A. S. (1985) *Biochim. Biophys. Acta 817*, 193−196.
33. MacDonald, R. C., MacDonald, R. I., Menco, B. P. M., Takeshita, K., Subbarao, N. K., and Hu, L. (1991) *Biochim. Biophys. Acta 1061*, 297−303.
34. Chen, Y.-H., Yang, J. T., and Chau, K. H. (1974) *Biochemistry 13*, 3350−3359.
35. Rajasekharan, R., and Kemp, J. D. (1994) *J. Lipid Res. 35*, 45−51.
36. Ball, E. H. (1986) *Anal. Biochem. 155*, 23−27.
37. Bonner, W. M., and Laskey, R. A. (1974) *Eur. J. Biochem. 46*, 83−88.
38. Williams, R. W., Starman, R., Taylor, K. M. P., Gable, K., Beeler, T., Zasloff, M., and Covell, D. (1990) *Biochemistry 29*, 4490−4496.
39. Gupta, C. M., Costello, C. E., and Khorana, G. (1979) *Proc. Natl. Acad. Sci. U.S.A. 76*, 3139−3143.
40. Brunner, J., and Richards, F. M. (1980) *J. Biol. Chem. 255*, 3319−3329.
41. LaTorre, R., Miller, C. G., and Quay, S. (1981) *Biophys. J. 36*, 803−809.
42. He, K., Ludtke, S. J., Heller, W. T., and Huang, H. W. (1996) *Biophys. J. 71*, 2669−2679.
43. Wu, Y., He, K., Ludtke, S. J., and Huang, H. W. (1995) *Biophys. J. 68*, 2361−2369.
44. Abrams, F. S., and London, E. (1992) *Biochemistry 31*, 5312−5322.
45. Brasseur, R. (1991) *J. Biol. Chem. 266*, 16120−16127.
46. Schwarz, G., Stankowski, S., and Rizzo, V. (1986) *Biochim. Biophys. Acta 861*, 141−151.
47. Matsuzaki, K., Nakamura, A., Murase, O., Sugishita, K., Fujii, N., and Miyajima, K. (1997) *Biochemistry 36*, 2104−2111.
48. Bechinger, B. (1997) *J. Membr. Biol. 156*, 197−211.
49. Wenk, M. K., and Seelig, J. (1998) *Biochemistry 37*, 3909−3916.
50. Boggs, J. M., and Moscarello, M. A. (1978) *J. Membr. Biol. 39*, 75−96.
51. Cheifetz, S., Moscarello, M. A., and Deber, C. M. (1984) *Arch. Biochem. Bioophys. 233*, 151−160.

BI980855C